HHS Public Access

Author manuscript

J Immunol. Author manuscript; available in PMC 2018 August 15.

Published in final edited form as:

J Immunol. 2017 August 15; 199(4): 1261–1274. doi:10.4049/jimmunol.1700099.

A novel subset of anti-inflammatory CD138+ macrophages is deficient in mice with experimental lupus*

Shuhong Han[*], **Haoyang Zhuang**[*], **Stepan Shumyak**[*], **Jingfan Wu**[*], **Hui Li**[†], **Li-Jun Yang**[†], and **Westley H. Reeves**[*,2]

[*]Division of Rheumatology & Clinical Immunology, Department of Medicine, University of Florida, PO Box 100221, Gainesville, FL 32610-0221

[†]Department of Pathology, Immunology, & Laboratory Medicine, University of Florida, Gainesville, FL 32610

Abstract

Dead cells accumulating in the tissues may contribute to chronic inflammation. We examined the cause of impaired apoptotic cell clearance human and murine lupus. Dead cells accumulated in bone marrow from lupus patients but not from non-autoimmune patients undergoing myeloablation, where they were efficiently removed by macrophages. Impaired apoptotic cell uptake by macrophages also was seen in mice treated i.p. with pristane (develop lupus) but not mineral oil (MO, do not develop lupus). The inflammatory response to both pristane and MO rapidly depleted resident ($Tim4^+$) large peritoneal macrophages (LPM). The peritoneal exudate of pristane-treated mice contained mainly $Ly6C^{hi}$ inflammatory monocytes, whereas in MO-treated mice, it consisted predominantly of a novel subset of highly phagocytic macrophages resembling small peritoneal macrophages (SPM) that expressed $CD138^+$ and the scavenger receptor Marco. Treatment with anti-Marco neutralizing antibodies and the class A scavenger receptor antagonist polyinosinic acid inhibited phagocytosis of apoptotic cells by $CD138^+$ macrophages. $CD138^+$ macrophages expressed IL-10 receptor, CD206, and CCR2 but little TNFα or CX3CR1. They also expressed high levels of activated CREB, a transcription factor implicated in generating alternatively activated macrophages. Similar cells were identified in the spleen and lung of MO-treated mice and also were induced by lipopolysaccharide. We conclude that highly phagocytic, $CD138^+$ SPM-like cells with an anti-inflammatory phenotype may promote the resolution of inflammation in lupus and infectious diseases. These SPM-like cells are not restricted to the peritoneum, and may help clear apoptotic cells from tissues such as the lung, helping to prevent chronic inflammation.

Introduction

Macrophages (Mϕ) play a key role in the non-inflammatory disposal of apoptotic cells (1). Monocyte-derived Mϕ from SLE patients are poorly phagocytic (2) and patients accumulate apoptotic cells in their tissues (3–6). Dead cells also accumulate in tissues of mice with

[2]Correspondence to: Westley H. Reeves, M.D., Division of Rheumatology & Clinical Immunology, University of Florida, PO Box 100221, Gainesville, FL 32610-0221, Phone: 352-294-8200; Fax: 352-294-8204; whreeves@ufl.edu.

pristane-induced lupus (6), but not in mice treated with mineral oil (MO), an inflammatory hydrocarbon that does not cause lupus. Impaired phagocytosis of apoptotic cells promotes murine lupus (7–9). Although phagocytosis is usually non-inflammatory (8, 9), impaired phagocytosis of dead cells in lupus facilitates endosomal recognition of self-nucleic acids by TLR7 and TLR9, resulting in proinflammatory cytokine production (10). The outcome of phagocytosis (pro- vs. anti- inflammatory) depends on the release of damage-associated molecular patterns by dying cells, whether the cells are apoptotic or necrotic, the type of phagocyte, receptors mediating uptake, and factors regulating the sorting of apoptotic cells after phagocytosis or the coupling of phagocytosis to anti-inflammatory pathways (11–14). By overwhelming normal clearance mechanisms, an increased rate of cell death also may promote lupus (15–19).

We show impaired clearance of dead cells by lupus bone marrow (BM) Mϕ and report a novel subset of peritoneal $CD138^+$ Mϕ with an anti-inflammatory phenotype that efficiently takes up apoptotic cells in the peritoneum. This subset is deficient in mice with pristane-induced lupus, resulting in impaired apoptotic cell clearance and inflammation.

Materials and Methods

Patients

BM core biopsies were identified from the UF Department of Pathology archives. SLE was classified using ACR criteria (20, 21). Biopsies from adults with acute myelogenous leukemia (AML) undergoing myeloablation with cytarabine plus daunorubicin 14-days earlier and children with B cell acute lymphocytic leukemia (B-ALL) treated with vincristine, prednisone, anthracycline, plus cyclophosphamide and/or L-asparaginase 8-days earlier were de-identified and examined by H&E staining and immunohistochemistry (IHC). The patients were not treated with radiation and did not receive cytokines/growth factors in the week before bone marrow biopsy. Biopsies in which marrow cellularity dropped from 100% to <5% following myeloablation were selected for further study (n = 4). BM biopsies from patients undergoing myeloablation were compared with biopsies from SLE patients (n = 6) and controls undergoing BM biopsy for staging of lymphoma who had no evidence of BM involvement (n = 6). The UF IRB approved these studies.

IHC

BM core biopsies were fixed in 10% neutral buffered formalin and decalcified (6). Four-μm sections were deparaffinized and underwent heat-induced epitope retrieval before staining with anti-cleaved-caspase-3 (Cell Signaling), anti-TNFα (Abcam), and anti-CD68 (Dako) antibodies followed by peroxidase- or alkaline phosphatase-conjugated goat secondary antibodies (6). Reaction product was visualized using Ultra View DAB (brown) or Alkaline Phosphatase Red kits (Ventana). Slides were counterstained with hematoxylin. Numbers of activated caspase-3^+ cells (red) that did not co-localize with macrophages (brown) were determined as the mean number of red^+brown^- cells per 100X field (4 fields per patient).

Mice

Mice were maintained under specific pathogen-free conditions at the UF Animal Facility. C57BL/6 (B6) mice (Jackson Laboratory) received 0.5 mL of pristane (Sigma), mineral oil (MO, C.B. Fleet Co.), 100 ng lipopolysaccharide (LPS) from *Salmonella enterica* serotype Minnesota (Sigma), or PBS i.p. At indicated times, peritoneal exudate cells (PEC) were collected by lavage. Cells were analyzed within 1-hour. Bronchoalveolar lavage (BAL) was performed after euthanizing the mice. A small incision was cut in the trachea and 1-ml PBS was injected using a 20G plastic feeding tube (Instech Laboratories). Lung washings were analyzed within 1-hour. Animal studies were approved by the UF IACUC.

Quantitative PCR (Q-PCR)

Q-PCR was performed as described (6) using RNA extracted from 10^6 peritoneal cells (RNA isolation kit, Qiagen). cDNA was synthesized using the Superscript II First-Strand Synthesis kit (Invitrogen) and SYBR Green Q-PCR analysis was performed using an Opticon II thermocycler (Bio-Rad). Primer sequences were: *Mertk* forward GAGACCTCCACACCTTCCTG, reverse GAGCTGCCAAATCCCTATGA; *Sra1* forward CAACATCACCAACGACCTCA, reverse TGTCTCCCTTTTCACCTTGG; *Marco* forward AGCCGATTTTGACCAAGCTA, reverse, GTGAGCAGGATCAGGTGGAT; *Srb1* forward CCGAGAGTCTGGCATTCAG, reverse TGGGTTAGGGTTCAGACCAA; *Gata6* forward TACAAGAACACCAACACAGTCC, reverse GGCGTCAAGAGTGTTACAGATAC; *Pparg* forward CAAGGTGCTCCAGAAGATGA, reverse GTG AAGGCTCATGTCTGTCT; *Runx3* forward CGTGTAACACCAAGCACACC, reverse AAGGGGTTCAGGTCTGAGGA; *Car4* forward ACCTCTGACCTCAGCCTTTA, reverse CCACAGCCAGTTCCTCATATT; *Alox15* forward GCTTTCCATAGTCTGCTGTAGT, reverse TTTCCCAAGCATGGCTATTATTTAC; *β-actin* forward 5′-TGGAATCCTGTGGCATCCTGAAAC-3′, reverse 5′-TAAAACGCAGCTCAGTAACAGTCCG-3′.

Flow cytometry and cell sorting

Flow cytometry was performed as described (6). Cells were incubated with anti-mouse CD16/32 (Fc Block; BD Biosciences) before staining with primary antibody or isotype controls. Ten-thousand to 50,000 events per sample were acquired using an LSRII flow cytometer (BD-Biosciences) and analyzed with Flowjo flow cytometry software (Tree Star Inc.). The following antibodies were used: CD11b-Brilliant Violet 421, Tim4-PE, CD138-APC, CD138-PE F4/80- Pacific Blue, Ly6G-APC-Cy7, Ly6C-APC-Cy7, CD80-PerCp-Cy5, CD40-PerCP-Cy5, CD206- PerCP-Cy5, CCR2-FITC, CX3CR1-FITC, CD169-APC, CCR5-APC, CD36-PE, CD36-AlexaFluor 488, and IL-10R-PE (Biolegend); Marco-FITC (Biorad); Ly6C-FITC, CD86-FITC, CD11c-FITC, I-A/I-E-PE, CD93-PE (BD Bioscience); CREB-PE and Phospho-CREB-FITC (Cell Signaling); CD11b-Pacific Blue, CD45-FITC, TLR4-PE, CD45-FITC (eBioscience). Buffers used in intracellular staining were from eBioscience. For cell-sorting, PEC from untreated B6 mice were stained with anti-CD11b, Tim4, and CD138 antibodies. $CD11b^+Tim4^+$ and $CD11b^+CD138^+$ cells were gated and sorted (FACSaria cell sorter). Forty-thousand cells/subset were collected and lysed immediately for RNA extraction.

Phagocytosis of apoptotic cells and polystyrene beads

Mouse thymus lymphoma cells (BW5147) were induced into apoptosis by heat shock (45°C, 10-min) and cultured for 4-hr (22). The percentage of apoptotic (annexin-V^+) cells was routinely > 80% by this technique. After inducing apoptosis, cells were washed twice and labeled with pHrodo-Red (Life Technologies) (23). Uptake of labeled apoptotic cells was assayed *in vitro* by adding 10^6 apoptotic cells in AIM-V medium to each well of 12-well plate containing 10^6 adherent peritoneal cells. Plates were incubated 2.5-hours at 37°C, washed three times with ice cold PBS, and stained with Pacific blue-conjugated rat anti-mouse CD11b antibody (30-min, 4°C). Cells were washed again, detached with 1-ml ice-cold PBS using a cell scraper, and fixed with 1% paraformaldehyde before flow cytometry.

For *in vivo* assays, 2 X 10^7 pHrodo-red-labeled apoptotic cells were injected i.p. into pristane- or MO-treated mice (1-wk after treatment). After 1.5-hours, PEC were collected by lavage, stained with fluorescently-labeled anti-CD11b, anti-Ly6C, anti-CD138, and anti-Ly6G antibodies, washed and fixed as above.

To assess the role of Marco in apoptotic cell uptake, IgG anti-Marco neutralizing antibody (ED-31, AbD Serotec) or isotype control were injected i.p. into MO-treated mice (100-μg/mouse). Thirty minutes later, pHrodo-red labeled apoptotic cells were injected and uptake was determined 1.5-hours later as above. The Class A scavenger receptor inhibitor poly-inosinic acid (Poly-I) (Sigma) was used to further confirm the role of Marco. Poly-I (200 μg/mouse) or PBS was injected i.p and 30-min later, pHrodo-red labeled apoptotic BW5147 cells were injected. Uptake was measured by flow cytometry 1.5-hours later.

In vitro phagocytosis of unopsonized polystyrene beads (3.2 μm diameter) was measured by flow cytometry. Peritoneal exudate cells were obtained 1-wk after MO-treatment and cultured for 1-h with PE-labeled polystyrene beads at a 10:1 bead:cell ratio (DakoCytomation). Cells then were stained with anti-CD11b, Ly6C, Ly6G, and CD138 antibodies. The percentage of $CD11b^+Ly6G^-$ $Ly6C^-$ $CD138^+$ and $CD11b^+Ly6G^-$ $Ly6C^-$ $CD138^-$ cells that had taken up PE-labeled beads was determined by flow cytometry.

CREB activation

Peritoneal cells from untreated mice were incubated with PBS or LPS (100 ng/ml) for 30 min. Total CREB and phosphorylated CREB (p-CREB) staining was determined by flow cytometry in the $CD11b^+CD138^+Tim4^-$, $CD11b^+CD138^-$ $Tim4^+$, and $CD11b^+CD138^-$ $Ly6C^{hi}$ subsets. In some experiments mice were treated with the cell-permeable adenylate cyclase inhibitor SQ22536 (24). Mice received MO (0.5 ml i.p.) on day 1, and SQ22536 (250 μg/day i.p) (25) for 9-days starting on day 1. Peritoneal cells were analyzed by flow cytometry at day 9.

Statistical analysis

Statistical analyses were performed using Prism 6.0 software (GraphPad Software). Differences between groups were analyzed by unpaired Student *t* test (normally distributed data) or Mann-Whitney *U* test (non-normally distributed data). Data are expressed as mean ±

SD for normally distributed data sets. Normality was determined by the D'agostino and Person omnibus test. All tests were two-sided; $p < 0.05$ was considered significant.

Results

Dead cells accumulate in BM and lung tissue of mice with pristane-induced lupus and SLE patients and TNFα is produced locally (6, 26). To see if these abnormalities are associated with a phagocytosis defect, we compared BM from SLE patients and controls.

Impaired clearance of dead cells by human lupus Mϕ

SLE BM contained cells staining with antibodies against activated caspase-3, an apoptosis marker (Fig. 1A, middle). In contrast, caspase-3^+ cells were largely absent in BM from a non-SLE control (Fig. 1A, left). Wright staining also showed numerous dead cells in patients' BM aspirates (Fig. 1A, right).

To assess the clearance of dead cells, we studied patients undergoing myeloablative therapy for AML and B-ALL, which causes massive death of BM cells (27). BM from a child with B-ALL exhibited 100% cellularity prior to myeloablative therapy, but 8-days later was hypocellular (<5% cellularity) with erythroid regeneration (Fig. 1B). Large phagocytic cells, probably resident BM Mϕ, were visualized in the hypocellular marrow by H&E staining and IHC showed activated caspase-3 stained material within endosomes/phagosomes (Fig. 1B). Similar results were obtained using day-14 BM from AML patients (not shown). Caspase-3^+ material was restricted to endosomes/phagosomes of $CD68^+$ Mϕ (Fig. 1C, top left), whereas in SLE patients activated caspase-3 was found in intact cells located outside of $CD68^+$ BM Mϕ (Fig. 1C, right). Quantification of the number of caspase-3^+ cells outside of $CD68^+$ Mϕ confirmed that dead (caspase-3^+) cells were removed inefficiently in SLE BM vs. BM from non-SLE patients undergoing myeloablative therapy ($P < 0.01$, Student t-test) (Fig. 1D). There was no significant difference in caspase-3^+ cells in BM from myeloablated patients vs. untreated controls. Human lupus BM also stained prominently for TNFα (Fig. 1E, bottom right) (6), while TNFα was undetectable in BM from B-ALL 8-days after myeloablation (Fig. 1E, bottom left). Thus, non-lupus BM has an enormous capacity to clear dead cells but clearance is impaired and there is TNFα production in BM from SLE patients (Fig. 1) and pristane-treated mice (6). To explore the mechanism, we assessed the clearance of dead cells in pristane-induced lupus.

Impaired clearance of dead cells in pristane-induced lupus

In vitro phagocytosis assays revealed that $CD11b^+$ PEC from MO-treated mice took up 2.5-fold more apoptotic cells than $CD11b^+$ PEC from pristane-treated mice ($p<0.01$, Student t-test) (Fig. 2A). The mean fluorescence intensity (MFI) of pHrodo red in $CD11b^+$ cells also was lower in pristane- vs. MO-treated mice. Because *in vitro* culture alters Mϕ function, *in vivo* phagocytosis was measured by injecting pHrodo red-labeled apoptotic cells into the peritoneum followed 1.5-hrs later by flow cytometry for internalized target cells. Consistent with the *in vitro* data, a higher proportion of $CD11b^+$ cells from MO-treated mice took up apoptotic target cells and the pHrodo-red MFI was higher in comparison with pristane-

treated mice (Fig. 2B). We conclude that the uptake of dead cells is impaired in pristane-induced lupus, as in SLE patients.

In nontreated mice, the peritoneum contains a population of large, strongly phagocytic $CD11b^{+}Tim4^{+}$ resident Mϕ (28). Since these cells disappear in certain forms of inflammation (29–31), we examined whether differences in their numbers might explain the impaired phagocytosis of apoptotic cells in pristane- vs. MO-treated mice. However, $CD11b^{+}Tim4^{+}$ resident Mϕ disappeared 7-d after i.p. injection of either pristane or MO (Fig. 2C). Thus, although $Tim4^{+}$ resident Mϕ are highly phagocytic, a differential effect of pristane and MO on this subset was unlikely to explain impaired phagocytosis of apoptotic cells in pristane-treated mice.

Peritoneum contains a population of phagocytic $CD138^{+}$ Mϕ distinct from resident Mϕ

In addition to resident Mϕ, normal peritoneum contains BM-derived Mϕ (32, 33). We found an unusual subset of $CD11b^{+}CD138^{+}$ cells in the peritoneum of mice treated with pristane or MO (Fig. 3). These cells were more numerous in MO- vs. pristane- or PBS-treated mice (Fig. 3A) and expanded after MO (and to a lesser degree pristane) treatment (Fig. 3B). In contrast, $CD11b^{+}Ly6C^{hi}$ (inflammatory) monocytes rapidly increased in both pristane- and MO- treated mice, but decreased substantially over 14-days in MO, but not pristane, treated mice. At 1-wk neutrophils increased to a similar degree in pristane- and MO-treated mice (not shown). Thus, MO-treated mice exhibited an increasing predominance of $CD11b^{+}CD138^{+}$ cells whereas in pristane-treated mice $CD11b^{+}Ly6C^{hi}$ cells predominated.

Although CD138 usually is thought of as a plasma cell marker, $CD11b^{+}CD138^{+}$ cells took up pHrodo red-labeled apoptotic cells more actively *in vivo* than $Tim4^{+}$ Mϕ from the same mouse (Fig. 3C). In addition, *in vivo* uptake of apoptotic targets by $CD11b^{+}Tim4^{-}$ $CD138^{+}$ cells was considerably higher than that of $CD11b^{+}Tim4^{-}$ $CD138^{-}$ cells ($p<0.001$, Student t-test) (Fig. 3D). Flow cytometry of PEC from MO-treated mice revealed four subsets of $CD11b^{+}$ cells, best visualized in BALB/c mice but also seen in B6 mice (Fig. 3E): $CD11b^{+}Ly6C^{hi}$ (R1), $CD11b^{lo}Ly6C^{neg}$ (R2), $CD11b^{hi}Ly6C^{lo/-}$ (R3), and $CD11b^{+}Ly6C^{int}$ neutrophils, which also were $Ly6G^{+}$ (not shown). The main subset expressing CD138 was R3, which also expressed the Mϕ-restricted scavenger receptor Marco (Fig. 3E). $CD138^{+}Marco^{+}$ cells (R3) were considerably more phagocytic for apoptotic cells than other subsets (Fig. 3F).

In addition, we incubated peritoneal cells from 1-wk MO-treated mice for 1-h with PE-labeled polystyrene beads (3.2 μm, bead:cell ratio 10:1) and measured uptake by flow cytometry. Unopsonized polystyrene particles with a diameter >0.5 μm are taken up via Marco-mediated phagocytosis, whereas smaller particles are endocytosed (34). $CD11b^{+}CD138^{+}$ cells took up the beads more actively than $CD11b^{+}CD138^{-}$ cells (13.2% of cells vs. 5.4%, $P < 0.001$, Student t-test) (data not shown), suggesting that the high phagocytic activity of $CD11b^{+}CD138^{+}$ is not limited to uptake of apoptotic cells. However, the uptake of polystyrene particles was less efficient than uptake of apoptotic cells (Figs. 2–3).

Levels of *Marco* mRNA, encoding a class A scavenger receptor involved in uptake of apoptotic cells (35), was increased in PEC from MO- vs. pristane-treated mice ($P<0.005$, Student t-test). Expression of the class B scavenger receptor *Srb1* also was increased ($P<0.02$). In contrast, levels of *Mertk* and *Sra1* mRNA were comparable (Fig. 3G). The role of Marco in clearing apoptotic cells was examined by treating mice with MO followed by i.p. injection of anti-Marco neutralizing antibodies or isotype control before measuring *in vivo* phagocytosis (Fig. 3H, left). Blocking Marco inhibited apoptotic cell uptake, suggesting that Marco is involved in internalization. Peritoneal injection of the class A scavenger receptor antagonist poly(I) also inhibited uptake of labeled targets by $CD11b^+$ cells (Fig. 3H, right). Taken together, the data suggest that impaired phagocytosis of apoptotic cells in pristane- vs. MO- treated mice may reflect the relative numbers of highly phagocytic $CD11b^+CD138^+$ cells and expression of Marco and possibly other scavenger receptors by these cells promotes the clearance of dead cells. In contrast to the disappearance of $Tim4^+$ resident Mϕ, $CD11b^+CD138^+$ cells expanded during inflammation. Although $CD11b^+CD138^+$ cells have been reported (36), relatively little is known about them.

$CD11b^+CD138^+$ cells resemble small peritoneal macrophages (SPM)

The peritoneum contains two distinct subsets of Mϕ: resident "large peritoneal Mϕ" (LPM) and BM-derived "small peritoneal Mϕ" (SPM). The relationship of the $Tim4^+$ Mϕ and $CD11b^+CD138^+$ cells in the peritoneum of untreated mice to LPM and SPM was examined by gating on $CD11b^+$ cells and comparing surface-staining characteristics of the $Tim4^+$ vs. $CD11b^+CD138^+$ cells (Fig. 4A). $Tim4^+$ Mϕ expressed more CX3CR1 than $CD11b^+CD138^+$ cells and expressed both CD169 (Siglec-1) and CD93, which were nearly undetectable on $CD11b^+CD138^+$ cells (Fig. 4A). In contrast, $CD11b^+CD138^+$ cells expressed more CCR2, CCR5, and MHCII than $Tim4^+$ Mϕ and also expressed CD11c, which was absent on $Tim4^+$ Mϕ. The two subsets exhibited similar forward scatter, but side scatter was lower in the $CD11b^+CD138^+$ subset (Fig. 4B). The surface staining and forward/side scatter properties of $CD11b^+CD138^+$ cells are similar to those reported for SPM (33).

Peritoneal cells from untreated B6 mice were stained with antibodies to F4/80, CD11b, Tim4, and CD138 (Fig. 4C). About 60% of peritoneal $CD11b^+$ cells were $Tim4^+CD138^-$ resident Mϕ, whereas ~10% were $CD138^+Tim4^-$, and ~30% were $Tim4^-$ $CD138^-$. Consistent with the high expression of F4/80 on resident peritoneal Mϕ (32), the $Tim4^+CD138^-$ cells were $F4/80^{hi}$. In contrast, the $CD138^+Tim4^-$ subset was $F4/80^{int}$ (Fig. 4C). Gene expression differed in flow-sorted peritoneal $CD11b^+F4/80^{hi}CD138^-$ $Tim4^+$ resident Mϕ vs. the $CD11b^+F4/80^{int}CD138^+Tim4^-$ subset ("$CD138^+$ Mϕ") from untreated mice (Fig. 4D). In comparison with $Tim4^+$ Mϕ, $CD138^+$ Mϕ expressed little *Gata6* (specific for resident peritoneal Mϕ), *Pparg* (inducible in peritoneal Mϕ), *Runx3*, and *Car4* (inducible in peritoneal Mϕ). *Alox15* encodes 12/15-lipoxygenase, an enzyme involved in non-inflammatory clearance of apoptotic cells by resident peritoneal Mϕ (13, 37) and resolution phase Mϕ (38). It is up-regulated by the uptake of apoptotic cells (39). However, although high levels were found in the $Tim4^+$ Mϕ subset, $CD138^+$ Mϕ expressed little *Alox15* mRNA (Fig. 4D). In contrast, $CD138^+$ Mϕ expressed higher levels of *Marco* mRNA than $Tim4^+$ Mϕ.

CD138$^+$ Mϕ are not restricted to the peritoneum

Although present in the peritoneum, CD138$^+$ Mϕ also were found in spleen from MO-treated and (in low numbers) pristane-treated mice (Fig. 5A). They were absent in spleen from PBS treated mice (Fig. 5A). Spleen contains CD138$^+$ plasma cells, but the CD138$^+$CD11b$^+$ population expressed CD36, F4/80, CD80, IL-10R, and Ly6C (Fig. 5B), verifying that these were CD138$^+$ Mϕ. CD138$^+$ Mϕ were present at low levels in BM from PBS-treated mice and did not change after pristane or MO treatment (Fig. 5C). Analysis of cells collected by BAL from MO-treated mice revealed two populations of F4/80$^+$CD11b$^+$ lung Mϕ: large CD138^{lo}Ly6C^{lo} Mϕ (R2) and smaller CD138^{hi}Ly6C^{hi} Mϕ (R1) (Fig. 5D). Both expressed IL10R, but expression was higher in R1. The large (R2) cells are likely to be alveolar Mϕ, whereas the small cells are similar to peritoneal CD138$^+$ Mϕ (but expressed higher levels of Ly6C than peritoneal CD138$^+$ Mϕ). BAL from pristane- or PBS-treated mice contained few CD138$^+$ Mϕ (not shown). Thus, CD138$^+$ Mϕ are not restricted to the peritoneum and may develop from CD138$^-$ BM precursors upon migration to sites of inflammation.

CD138$^+$ Mϕ are induced by LPS

To see if the induction of CD138$^+$ Mϕ is relevant to infection, mice received LPS (100 ng i.p.) and PEC were analyzed by flow cytometry. At 7-days the peritoneum of LPS-treated mice contained variable numbers of Ly6G$^+$ neutrophils and 20–40% CD138$^+$ Mϕ, but few (2–5%) Ly6C^{hi} inflammatory monocytes (Fig. 6A–B). LPS depleted Tim$^+$CD138$^-$ resident peritoneal Mϕ within 1-day (Fig. 6C). At 3-days, small numbers of Tim4$^+$ cells were detected in MO-treated mice and larger numbers in LPS-treated mice. Unexpectedly, at 7-days, many Tim4$^+$ cells in LPS-treated, but not MO-treated mice, were CD138$^+$. At 14–28 days, MO-treated mice also had peritoneal Tim4$^+$CD138$^+$ cells (Fig. 6C). Tim4$^-$ CD138$^-$ cells were very poorly phagocytic for apoptotic cells, whereas Tim4$^+$CD138$^-$, Tim4$^+$CD138$^+$ and Tim4$^-$ CD138$^+$ cells all could up-take apoptotic cells (data not shown). However, there was not a significant difference in the ability of the three latter subsets to take up apoptotic cells.

CD138$^+$Tim4$^-$ Mϕ have an anti-inflammatory phenotype

CD138 (syndecan-1) is a transmembrane proteoglycan encoded by *Sdc1* (40). Although expressed mainly on epithelial, mesenchymal, and plasma cells, it also is found on monocytes (41). Peritoneal mBSA-induced F4/80^{int} Mϕ express CD138 and may promote the resolution of inflammation (42–44). Consistent with that possibility, IL-10 receptor (IL10R) surface staining was higher on CD138$^+$ Mϕ than on Ly6C^{hi} monocytes or CD138$^-$ Mϕ in both pristane- and MO-treated mice (Fig. 7A,B) and CD138$^+$ Mϕ exhibited lower intracellular TNFα staining than Ly6C^{hi} monocytes (Fig. 7C). CD138$^+$ Mϕ from untreated mice also expressed high levels of the M2 Mϕ marker CD206 (mannose receptor) and CD138$^-$ Tim4$^+$ resident Mϕ expressed lower levels (Fig. 7D). Thus, CD138$^+$ Mϕ have a phenotype (low TNFα production, high IL10R, and high CD206) suggestive of anti-inflammatory/resolution-phase Mϕ.

Like CD138$^+$ Mϕ, resolution-phase Mϕ express M2 markers, respond poorly to TLR ligands, and are highly phagocytic (39, 45). Since resolution-phase Mϕ markedly down-

regulate CD11b following the uptake of apoptotic cells *in vitro* (39), we examined CD11b expression on CD138$^+$ Mϕ. The expression level of CD11b was lower on CD138$^+$ Mϕ from MO- vs. pristane- treated mice (Fig. 7E, left). Following 20-h co-culture of CD138$^+$ Mϕ from MO-treated mice with apoptotic BW5147 cells (5:1 ratio of apoptotic targets to Mϕ), CD11b fluorescence intensity substantially decreased (Fig. 7E, right). Thus, like resolution phase Mϕ, CD138$^+$ Mϕ also down-regulate CD11b after taking up apoptotic cells. These data suggest that the improved phagocytic capacity in CD138$^+$ cells from MO-treated mice drives increased reprogramming to the CD11b^{low} phenotype.

Increased CREB activation in CD138$^+$ Mϕ

The phenotype of resolution-phase Mϕ is controlled by cAMP (45) and the cAMP/PKA-activated transcription factor CREB induces an anti-inflammatory gene expression program in Mϕ (46). As CD138 (*Sdc1*) is CREB-regulated (41), we investigated CREB activation in CD138$^+$ Mϕ. Total CREB levels were similar in CD11b$^+$CD138$^+$Tim4$^-$ and CD11b$^+$CD138$^-$ Tim4$^+$ Mϕ from untreated mice but activated CREB (p-CREB) was increased in CD11b$^+$CD138$^+$Tim4$^-$ Mϕ (Fig. 8A). CD11b$^+$CD138$^+$Tim4$^-$ Mϕ also expressed higher levels of p-CREB after LPS treatment (30-min *in vitro*). Similar to CD138$^+$ Mϕ, CD11b$^+$CD138$^-$ Tim4$^+$ resident Mϕ exhibited higher levels of p-CREB after LPS treatment. (Fig. 8B, left). Compared with Tim4$^+$ resident Mϕ, CD138$^+$ Mϕ from untreated mice expressed higher levels of p-CREB (Fig. 8B, right). Both phosphorylated and total CREB were higher in CD138$^+$ Mϕ vs. Ly6C^{hi} monocytes (Fig. 8C). CD11b$^+$CD138$^+$ peritoneal Mϕ from mice treated daily with the adenylate cyclase inhibitor SQ22536 had higher surface Ly6C staining than controls and produced more TNFα (intracellular staining), suggesting that treatment promoted a pro-inflammatory phenotype (Fig. 8D). SQ22536 treatment had no significant effect on either the fluorescence intensity of CD138 staining or the percentage of CD138$^+$ Mϕ (not shown).

Discussion

Phagocytosis of apoptotic cells by SLE patients' monocytes is impaired *in vitro* (2) and dead cells accumulate in their tissues (3–5) and also in tissues of mice with pristane-induced lupus (6, 47). The present study suggests that the accumulation of dead cells occurs in the setting of impaired clearance by Mϕ. Reduced clearance of apoptotic cells in lupus mice was associated with low numbers of a novel subset of CD138$^+$ Mϕ that was highly phagocytic for apoptotic cells and had an anti-inflammatory phenotype. Phagocytosis was mediated partly by the scavenger receptor Marco. CREB, which regulates CD138 expression and induces an anti-inflammatory transcriptional program, was activated in these CD138$^+$ Mϕ (41, 46, 48).

Impaired phagocytosis of dead cells in lupus

Most tissues contain self-renewing resident Mϕ derived from embryonic precursors that seed the tissues before birth (49–51). During inflammation, resident Mϕ are transiently complemented by short-lived recruited monocytes that differentiate *in situ* into Mϕ (49). The accumulation of dead cells in patients' tissues (3–6) suggests that phagocytosis is abnormal, cell death is increased, or both. Cell death is increased in SLE patients (15–17)

and mice with pristane-induced lupus (18, 19). But dead cells were efficiently cleared by BM Mϕ in non-lupus patients undergoing myeloablative therapy without triggering TNFα production (Fig. 1), consistent with other evidence that apoptotic cells are cleared efficiently without inducing inflammation (52). In contrast, dead cells accumulate in lupus BM and induce local TNFα production [(Fig. 1); (6)]. In pristane-induced lupus, phagocytosis of apoptotic cells was impaired *in vitro* and *in vivo* (Fig. 2). This was not seen in mice treated with MO, an inflammatory, but non-lupus-inducing hydrocarbon oil. Defective apoptotic cell removal may contribute to the pathogenesis of lupus by activating innate immunity (7).

Pristane impairs generation of Mϕ that clear apoptotic cells

$CD11b^{+}Tim4^{+}$ resident peritoneal Mϕ, which actively take up apoptotic cells, were reduced >90% shortly after pristane or MO treatment, consistent with prior studies showing that peritoneal inflammation rapidly depletes resident peritoneal Mϕ (29, 53). This "Mϕ disappearance reaction" (31) is caused by re-localization of $CD11b^{+}Tim4^{+}$ ($Gata6^{+}$) resident peritoneal Mϕ to omental milky spots (30). $CD138^{+}$ Mϕ were more active than $CD11b^{+}Tim4^{+}$ Mϕ at taking up apoptotic cells and were not depleted by peritoneal inflammation, but were affected differentially by pristane and MO. In MO-treated mice, $CD138^{+}$ Mϕ expanded and $Ly6C^{hi}$ monocytes decreased, whereas high levels of $Ly6C^{hi}$ monocytes and lower levels of $CD138^{+}$ Mϕ were maintained in pristane-treated mice (Fig. 3). $CD138^{+}$ Mϕ were the most active peritoneal myeloid subset at taking up apoptotic cells and their relative deficiency may explain the decreased clearance of apoptotic cells in pristane- vs. MO-treated mice. $CD138^{+}$ Mϕ were not unique to pristane/MO-induced inflammation, as they appeared in the peritoneum 7-days after LPS treatment (Fig. 6). Thus, $CD138^{+}$ Mϕ may play a physiological role in resolving infectious as well as sterile inflammation, possibly by promoting clearance of dead cells.

Role of scavenger receptors in $CD138^{+}$ Mϕ

Impaired phagocytosis of apoptotic cells promotes murine lupus (7). Two phagocytic processes remove dead cells: opsonin-dependent (e.g. Fc receptors, complement receptors, TAM receptors) and opsonin-independent (including phosphatidylserine receptors, such as Tim-4) (9). Opsonins such as MFG-E8, Gas6, and protein S are involved in the recognition of apoptotic cells by integrins and the TAM receptors (54–56). This plays a major role in clearing apoptotic cells. In contrast, Marco and other scavenger receptors recognize oxidized LDL on the surface of apoptotic cells without a requirement for opsonization, promoting their clearance and inhibiting cytokine/chemokine responses (35, 57, 58). $CD138^{+}$ Mϕ expressed the class A scavenger receptor Marco and class B scavenger receptors SR-B1 and CD36. Treatment with anti-Marco neutralizing antibodies or the class A scavenger receptor antagonist Poly(I) reduced phagocytosis of apoptotic cells by ~1/3 (Fig. 3), suggesting that clearance involves Marco. $CD138^{+}$ Mϕ also took up polystyrene particles more actively than $CD138^{-}$ Mϕ. Consistent with the role of Marco in clearing apoptotic cells, phagocytosis of unopsonized particles also is Marco-dependent (34).

Marco promotes non-inflammatory phagocytosis of apoptotic cells and is expressed constitutively on marginal zone Mϕ and some tissue Mϕ. It is induced on other Mϕ subsets via TLR signaling (9, 51). A Marco defect contributes to lupus in BXSB male mice (59),

and autoantibodies against Marco impair apoptotic cell uptake in murine and human lupus (60, 61). Moreover, anti-DNA autoantibody production is increased in Marco-deficient mice following injection of apoptotic cells (60). Our data support the idea that Marco deficiency promotes lupus. Expression of SR-B1 also was low in pristane-treated mice (Fig. 3). Since human SR-B1 recognizes apoptotic cells (62), it will be of interest to see if it plays a similar role in mice.

CD138$^+$ Mϕ resemble SPM

Normal peritoneum contains a major population of large, self-renewing resident Mϕ (LPM) established during fetal life and a minor (~10%) population of small, BM-derived Mϕ (SPM) (33). *Gata6*, a master transcriptional regulator of resident peritoneal Mϕ (29, 30), was expressed at high levels by Tim4$^+$CD138$^-$ LPM, as expected (Fig. 4D). The near-absence of *Gata6* expression in Tim4$^-$ CD138$^+$ Mϕ and intermediate F4/80 staining (Fig. 4C) are consistent with BM-derived SPM (32, 33). Their surface phenotype further supports the close relationship of CD138$^+$ Mϕ to SPM (33). Both express high levels of MHCII and low/intermediate levels of F4/80, but not CD93 (AA4.1) or Ly6C (Fig. 4). In contrast to LPM, CD138$^+$ Mϕ (Figs. 2,3) and SPM (33) do not disappear from the peritoneum during inflammation. However, the kinetics of appearance/disappearance of F4/80^{hi}CD11b^{hi} (LPM-like) and F4/80^{int}CD11b^{int} (SPM-like) cells may vary depending on the model of peritoneal inflammation used (63).

In contrast to previous reports, our studies suggest that CD138$^+$ Mϕ/SPM are not restricted to the peritoneum, as they were detected in the spleen and lungs of pristane- and MO-treated mice (Fig. 5). They did not change in the BM after treatment, suggesting that CD138$^+$ Mϕ arise peripherally by differentiation of CD138$^-$ BM precursors. Ly6C^{hi} monocytes can give rise to SPM during inflammation, suggesting that Ly6C$^+$ cells expressing low levels of CD138 (Fig. 3E) and possibly the CD138$^+$Ly6C$^+$ lung Mϕ (Fig. 5D) are an intermediate stage in the differentiation of CD138$^+$Ly6C$^-$ Mϕ from CD138$^-$ Ly6C^{hi} precursors.

A population of CD138$^+$Tim4$^+$ Mϕ was found in LPS-treated mice (Fig. 6C) and similar cells appeared later on in MO-treated mice. These cells resemble a subset of alternatively-activated resident Mϕ (64). However, further studies are needed to confirm that they are not BM-derived.

CD138$^+$ Mϕ have an anti-inflammatory phenotype

Although an over-simplification (65), BM-derived Mϕ have been classified into two subtypes: M1 (classically activated, proinflammatory) and M2 (alternatively activated, associated with resolution). M1/M2 polarization is influenced by transcription factors (65, 66) and epigenetic regulation (67). Mouse M1 Mϕ express iNOS (*Nos2*) and high levels of Ly6C, MHCII, and CCR2 and produce TNFα, IL-1β, and IL-12, whereas M2 Mϕ express arginase 1 (*Arg1*), scavenger receptors, CX3CR1, and low levels of Ly6C and produce TGFβ and IL-10 (67). CD138$^+$ Mϕ exhibited some features of both. Consistent with an M1 phenotype, they expressed high levels of MHCII and CCR2 and low levels of CX3CR1 (Fig. 4). But they were Ly6C$^-$ and expressed CD206 (Fig. 7), an “M2c” Mϕ marker expressed on BM-derived, but not resident, M2-like Mϕ (64, 68, 69). Moreover, like other pro-resolving

Mϕ (39), CD138^{+} Mϕ down-regulated CD11b, a component of complement receptor 3, following co-culture with apoptotic cells (Fig. 7E). In blood vessels, CD138^{+} Mϕ are anti-inflammatory (36). A CREB and cAMP/PKA-regulated transcriptional program controls *Sdc1* (CD138), *Klf4*, *Arg1*, *Il10*, and other genes involved in M2 polarization (41, 46, 48). The increased levels of p-CREB in CD138^{+} Mϕ and high levels of IL10R expression are consistent with an M2-like phenotype (Fig. 7). We speculate that the pattern of chemokine receptor expression (CCR2^{hi} CX$_3$CR1^{lo}) might allow anti-inflammatory CD138^{+} Mϕ to migrate to the same sites as proinflammatory Ly6C^{hi} (CCR2^{hi}) monocytes, promoting resolution of inflammation. Thus, CD138^{+} Mϕ exhibit several features of resolution-phase Mϕ, including an M2-like surface phenotype with some M1 markers, high phagocytic activity, and down-regulation of CD11b following the uptake of apoptotic cells (39, 45).

Finally, our studies suggest that the cAMP/protein kinase A (PKA)-regulated transcription factor CREB may help maintain the M2-like/pro-resolving phenotype of CD138^{+} Mϕ. The increased level of p-CREB in CD138^{+} Mϕ supports that possibility (Fig. 8). CREB activation promotes M2 polarization (46, 70) and the phenotype of resolution-phase Mϕ is controlled by cAMP (45). Although CD138 expression is regulated by cAMP/PKA and CREB (41), we did not see lower CD138 surface staining in mice treated with the adenylate cyclase inhibitor SQ22536 (data not shown). However, Ly6C staining and TNFα were increased, consistent with a shift toward M1-like polarization (Fig. 8D). It remains unclear whether CD138 is a component of a transcriptional program that dampens inflammatory responses (36) or only a marker for a subset of anti-inflammatory/resolution phase Mϕ. Inhibition of cyclic nucleotide phosphodiesterase type 4 (PDE4), which hydrolyzes cAMP, modulates disease progression in MRL/*lpr* lupus mice (71) and the PDE4 inhibitor apremilast is beneficial in human discoid lupus (72). It will be of interest in the future to see if PDE4 inhibitors promote expansion of the CD138^{+} Mϕ subset via CREB activation.

Acknowledgments

Supported by research grant R01-AR44731 from NIH/NIAMS and a grant from the Lupus Research Institute

References

1. Serhan CN, Savill J. Resolution of inflammation: the beginning programs the end. Nat Immunol. 2005; 6:1191–1197. [PubMed: 16369558]
2. Herrmann M, Voll RE, Zoller OM, Hagenhofer M, Ponner BB, Kalden JR. Impaired phagocytosis of apoptotic cell material by monocyte-derived macrophages from patients with systemic lupus erythematosus. Arthritis Rheum. 1998; 41:1241–1250. [PubMed: 9663482]
3. Baumann I, Kolowos W, Voll RE, Manger B, Gaipl U, Neuhuber WL, Kirchner T, Kalden JR, Herrmann M. Impaired uptake of apoptotic cells into tingible body macrophages in germinal centers of patients with systemic lupus erythematosus. Arthritis Rheum. 2002; 46:191–201. [PubMed: 11817590]
4. Jeruc J, Vizjak A, Rozman B, Ferluga D. Immunohistochemical expression of activated caspase-3 as a marker of apoptosis in glomeruli of human lupus nephritis. Am J Kidney Dis. 2006; 48:410–418. [PubMed: 16931214]
5. Makino H, Sugiyama H, Yamasaki Y, Maeshima Y, Wada J, Kashihara N. Glomerular cell apoptosis in human lupus nephritis. Virchows Archiv : an international journal of pathology. 2003; 443:67–77. [PubMed: 12750884]

6. Zhuang H, Han S, Xu Y, Li Y, Wang H, Yang LJ, Reeves WH. Toll-like receptor 7-stimulated tumor necrosis factor alpha causes bone marrow damage in systemic lupus erythematosus. Arthritis Rheumatol. 2014; 66:140–151. [PubMed: 24449581]
7. Nagata S, Hanayama R, Kawane K. Autoimmunity and the clearance of dead cells. Cell. 2010; 140:619–630. [PubMed: 20211132]
8. Voll RE, Herrmann M, Roth EA, Stach C, Kalden JR, Girkontaite I. Immunosuppressive effects of apoptotic cells. Nature. 1997; 390:350–351. [PubMed: 9389474]
9. Taylor PR, Martinez-Pomares L, Stacey M, Lin HH, Brown GD, Gordon S. Macrophage receptors and immune recognition. Annu Rev Immunol. 2005; 23:901–944. [PubMed: 15771589]
10. Marshak-Rothstein A. Toll-like receptors in systemic autoimmune disease. Nat Rev Immunol. 2006; 6:823–835. [PubMed: 17063184]
11. Green DR, Ferguson T, Zitvogel L, Kroemer G. Immunogenic and tolerogenic cell death. Nat Rev Immunol. 2009; 9:353–363. [PubMed: 19365408]
12. Dixon KO, O'Flynn J, van der Kooij SW, van Kooten C. Phagocytosis of apoptotic or necrotic cells differentially regulates the transcriptional expression of IL-12 family members in dendritic cells. J Leukoc Biol. 2014; 96:313–324. [PubMed: 24782489]
13. Uderhardt S, Herrmann M, Oskolkova OV, Aschermann S, Bicker W, Ipseiz N, Sarter K, Frey B, Rothe T, Voll R, Nimmerjahn F, Bochkov VN, Schett G, Kronke G. 12/15-lipoxygenase orchestrates the clearance of apoptotic cells and maintains immunologic tolerance. Immunity. 2012; 36:834–846. [PubMed: 22503541]
14. A-Gonzalez N, Bensinger SJ, Hong C, Beceiro S, Bradley MN, Zelcer N, Deniz J, Ramirez C, Diaz M, Gallardo G, de Galarreta CR, Salazar J, Lopez F, Edwards P, Parks J, Andujar M, Tontonoz P, Castrillo A. Apoptotic cells promote their own clearance and immune tolerance through activation of the nuclear receptor LXR. Immunity. 2009; 31:245–258. [PubMed: 19646905]
15. Fan H, Liu F, Dong G, Ren D, Xu Y, Dou J, Wang T, Sun L, Hou Y. Activation-induced necroptosis contributes to B-cell lymphopenia in active systemic lupus erythematosus. Cell Death Dis. 2014; 5:e1416. [PubMed: 25210799]
16. Souliotis VL, Sfikakis PP. Increased DNA double-strand breaks and enhanced apoptosis in patients with lupus nephritis. Lupus. 2015; 24:804–815. [PubMed: 25542905]
17. Colonna L, Lood C, Elkon KB. Beyond apoptosis in lupus. Curr Opin Rheumatol. 2014; 26:459–466. [PubMed: 25036095]
18. Calvani N, Caricchio R, Tucci M, Sobel ES, Silvestris F, Tartaglia P, Richards HB. Induction of apoptosis by the hydrocarbon oil pristane: implications for pristane-induced lupus. J Immunol. 2005; 175:4777–4782. [PubMed: 16177126]
19. Herman S, Kny A, Schorn C, Pfatschbacher J, Niederreiter B, Herrmann M, Holmdahl R, Steiner G, Hoffmann MH. Cell death and cytokine production induced by autoimmunogenic hydrocarbon oils. Autoimmunity. 2012; 45:602–611. [PubMed: 22917079]
20. Tan EM, Cohen AS, Fries JF, Masi AT, McShane DJ, Rothfield NF, Schaller JG, Talal N, Winchester RJ. The 1982 revised criteria for the classification of systemic lupus erythematosus. Arthritis Rheum. 1982; 25:1271–1277. [PubMed: 7138600]
21. Hochberg MC. Updating the American College of Rheumatology revised criteria for the classification of systemic lupus erythematosus. Arthritis Rheum. 1997; 40:1725.
22. Lee PY, Kumagai Y, Li Y, Takeuchi O, Yoshida H, Weinstein J, Kellner ES, Nacionales D, Barker T, Kelly-Scumpia K, van RN, Kumar H, Kawai T, Satoh M, Akira S, Reeves WH. TLR7-dependent and FcgammaR-independent production of type I interferon in experimental mouse lupus. J Exp Med. 2008; 205:2995–3006. [PubMed: 19047436]
23. Miksa M, Komura H, Wu R, Shah KG, Wang P. A novel method to determine the engulfment of apoptotic cells by macrophages using pHrodo succinimidyl ester. J Immunol Methods. 2009; 342:71–77. [PubMed: 19135446]
24. Pierre S, Eschenhagen T, Geisslinger G, Scholich K. Capturing adenylyl cyclases as potential drug targets. Nat Rev Drug Discov. 2009; 8:321–335. [PubMed: 19337273]

25. Imamura TK, Yoshino Y, Yamachika S, Ishii H, Watanabe NY, Inoue H, Nakagawa Y. Inhibition of pilocarpine-induced saliva secretion by adrenergic agonists in ICR mice. Clin Exp Pharmacol Physiol. 2012; 39:1038–1043. [PubMed: 23075092]
26. Zhuang H, Han S, Lee PY, Khaybullin R, Shumyak S, Lu L, Chatha A, Afaneh A, Zhang Y, Xie C, Nacionales D, Moldawer L, Qi X, Yang LJ, Reeves WH. Pathogenesis of diffuse alveolar hemorrhage in murine lupus. Arthritis Rheumatol. 2017; 69 In Press.
27. Villela L, Bolanos-Meade J. Acute myeloid leukaemia: optimal management and recent developments. Drugs. 2011; 71:1537–1550. [PubMed: 21861539]
28. Cain DW, O'Koren EG, Kan MJ, Womble M, Sempowski GD, Hopper K, Gunn MD, Kelsoe G. Identification of a tissue-specific, C/EBPbeta-dependent pathway of differentiation for murine peritoneal macrophages. J Immunol. 2013; 191:4665–4675. [PubMed: 24078688]
29. Rosas M, Davies LC, Giles PJ, Liao CT, Kharfan B, Stone TC, O'Donnell VB, Fraser DJ, Jones SA, Taylor PR. The transcription factor Gata6 links tissue macrophage phenotype and proliferative renewal. Science. 2014; 344:645–648. [PubMed: 24762537]
30. Okabe Y, Medzhitov R. Tissue-specific signals control reversible program of localization and functional polarization of macrophages. Cell. 2014; 157:832–844. [PubMed: 24792964]
31. Barth MW, Hendrzak JA, Melnicoff MJ, Morahan PS. Review of the macrophage disappearance reaction. J Leukoc Biol. 1995; 57:361–367. [PubMed: 7884305]
32. Leavy O. Macrophages: Peritoneal population depends on GATA6. Nat Rev Immunol. 2014; 14:360. [PubMed: 24854587]
33. Ghosn EE, Cassado AA, Govoni GR, Fukuhara T, Yang Y, Monack DM, Bortoluci KR, Almeida SR, Herzenberg LA, Herzenberg LA. Two physically, functionally, and developmentally distinct peritoneal macrophage subsets. Proc Natl Acad Sci USA. 2010; 107:2568–2573. [PubMed: 20133793]
34. Kanno S, Furuyama A, Hirano S. A murine scavenger receptor MARCO recognizes polystyrene nanoparticles. Toxicol Sci. 2007; 97:398–406. [PubMed: 17361018]
35. Platt N, Suzuki H, Kurihara Y, Kodama T, Gordon S. Role for the class A macrophage scavenger receptor in the phagocytosis of apoptotic thymocytes in vitro. Proc Natl Acad Sci USA. 1996; 93:12456–12460. [PubMed: 8901603]
36. Xiao J, Angsana J, Wen J, Smith SV, Park PW, Ford ML, Haller CA, Chaikof EL. Syndecan-1 displays a protective role in aortic aneurysm formation by modulating T cell-mediated responses. Arterioscler Thromb Vasc Biol. 2012; 32:386–396. [PubMed: 22173227]
37. Lavin Y, Winter D, Blecher-Gonen R, David E, Keren-Shaul H, Merad M, Jung S, Amit I. Tissue-resident macrophage enhancer landscapes are shaped by the local microenvironment. Cell. 2014; 159:1312–1326. [PubMed: 25480296]
38. Stables MJ, Shah S, Camon EB, Lovering RC, Newson J, Bystrom J, Farrow S, Gilroy DW. Transcriptomic analyses of murine resolution-phase macrophages. Blood. 2011; 118:e192–208. [PubMed: 22012065]
39. Schif-Zuck S, Gross N, Assi S, Rostoker R, Serhan CN, Ariel A. Saturated-efferocytosis generates pro-resolving CD11b low macrophages: modulation by resolvins and glucocorticoids. Eur J Immunol. 2011; 41:366–379. [PubMed: 21268007]
40. Akl MR, Nagpal P, Ayoub NM, Prabhu SA, Gliksman M, Tai B, Hatipoglu A, Goy A, Suh KS. Molecular and clinical profiles of syndecan-1 in solid and hematological cancer for prognosis and precision medicine. Oncotarget. 2015; 6:28693–28715. [PubMed: 26293675]
41. Kim C, Wilcox-Adelman S, Sano Y, Tang WJ, Collier RJ, Park JM. Antiinflammatory cAMP signaling and cell migration genes co-opted by the anthrax bacillus. Proc Natl Acad Sci USA. 2008; 105:6150–6155. [PubMed: 18427110]
42. Tomasdottir V, Vikingsson A, Hardardottir I, Freysdottir J. Murine antigen-induced inflammation--a model for studying induction, resolution and the adaptive phase of inflammation. J Immunol Methods. 2014; 415:36–45. [PubMed: 25268546]
43. Teng YH, Aquino RS, Park PW. Molecular functions of syndecan-1 in disease. Matrix Biol. 2012; 31:3–16. [PubMed: 22033227]
44. Yeaman C, Rapraeger AC. Post-transcriptional regulation of syndecan-1 expression by cAMP in peritoneal macrophages. J Cell Biol. 1993; 122:941–950. [PubMed: 8394371]

45. Bystrom J, Evans I, Newson J, Stables M, Toor I, van Rooijen N, Crawford M, Colville-Nash P, Farrow S, Gilroy DW. Resolution-phase macrophages possess a unique inflammatory phenotype that is controlled by cAMP. Blood. 2008; 112:4117–4127. [PubMed: 18779392]

46. Ruffell D, Mourkioti F, Gambardella A, Kirstetter P, Lopez RG, Rosenthal N, Nerlov C. A CREB-C/EBPbeta cascade induces M2 macrophage-specific gene expression and promotes muscle injury repair. Proc Natl Acad Sci USA. 2009; 106:17475–17480. [PubMed: 19805133]

47. Zhuang H, Han S, Li Y, Kienhöfer D, Lee P, Shumyak S, Meyerholz R, Rosadzinski K, Rosner D, Chan A, Xu Y, Segal M, Sobel E, Yang LJ, Hoffmann MH, Reeves WH. A novel mechanism for generating the interferon signature in lupus: opsonization of dead cells by complement and IgM. Arthritis Rheumatol. 2016; 68:2917–2928. [PubMed: 27274010]

48. Aronoff DM, Canetti C, Serezani CH, Luo M, Peters-Golden M. Cutting edge: macrophage inhibition by cyclic AMP (cAMP): differential roles of protein kinase A and exchange protein directly activated by cAMP-1. J Immunol. 2005; 174:595–599. [PubMed: 15634874]

49. Yona S, Kim KW, Wolf Y, Mildner A, Varol D, Breker M, Strauss-Ayali D, Viukov S, Guilliams M, Misharin A, Hume DA, Perlman H, Malissen B, Zelzer E, Jung S. Fate mapping reveals origins and dynamics of monocytes and tissue macrophages under homeostasis. Immunity. 2013; 38:79–91. [PubMed: 23273845]

50. Hashimoto D, Chow A, Noizat C, Teo P, Beasley MB, Leboeuf M, Becker CD, See P, Price J, Lucas D, Greter M, Mortha A, Boyer SW, Forsberg EC, Tanaka M, van Rooijen N, Garcia-Sastre A, Stanley ER, Ginhoux F, Frenette PS, Merad M. Tissue-resident macrophages self-maintain locally throughout adult life with minimal contribution from circulating monocytes. Immunity. 2013; 38:792–804. [PubMed: 23601688]

51. Ginhoux F, Jung S. Monocytes and macrophages: developmental pathways and tissue homeostasis. Nat Rev Immunol. 2014; 14:392–404. [PubMed: 24854589]

52. Henson PM, Bratton DL, Fadok VA. Apoptotic cell removal. Curr Biol. 2001; 11:R795–R805. [PubMed: 11591341]

53. Cassado Ados A, D'Imperio Lima MR, Bortoluci KR. Revisiting mouse peritoneal macrophages: heterogeneity, development, and function. Front Immunol. 2015; 6:225. [PubMed: 26042120]

54. Rothlin CV, Lemke G. TAM receptor signaling and autoimmune disease. Curr Opin Immunol. 2010; 22:740–746. [PubMed: 21030229]

55. Erwig LP, Henson PM. Clearance of apoptotic cells by phagocytes. Cell Death Differ. 2008; 15:243–250. [PubMed: 17571081]

56. Litvack ML, Palaniyar N. Review: Soluble innate immune pattern-recognition proteins for clearing dying cells and cellular components: implications on exacerbating or resolving inflammation. Innate Immun. 2010; 16:191–200. [PubMed: 20529971]

57. Wermeling F, Chen Y, Pikkarainen T, Scheynius A, Winqvist O, Izui S, Ravetch JV, Tryggvason K, Karlsson MC. Class A scavenger receptors regulate tolerance against apoptotic cells, and autoantibodies against these receptors are predictive of systemic lupus. J Exp Med. 2007; 204:2259–2265. [PubMed: 17893199]

58. Greaves DR, Gordon S. The macrophage scavenger receptor at 30 years of age: current knowledge and future challenges. J Lipid Res. 2009; 50(Suppl):S282–286. [PubMed: 19074372]

59. Rogers NJ, Lees MJ, Gabriel L, Maniati E, Rose SJ, Potter PK, Morley BJ. A defect in Marco expression contributes to systemic lupus erythematosus development via failure to clear apoptotic cells. J Immunol. 2009; 182:1982–1990. [PubMed: 19201851]

60. Wermeling F, Chen Y, Pikkarainen T, Scheynius A, Winqvist O, Izui S, Ravetch JV, Tryggvason K, Karlsson MC. Class A scavenger receptors regulate tolerance against apoptotic cells, and autoantibodies against these receptors are predictive of systemic lupus. J Exp Med. 2007; 204:2259–2265. [PubMed: 17893199]

61. Chen XW, Shen Y, Sun CY, Wu FX, Chen Y, Yang CD. Anti-class a scavenger receptor autoantibodies from systemic lupus erythematosus patients impair phagocytic clearance of apoptotic cells by macrophages in vitro. Arthritis Res Ther. 2011; 13:R9. [PubMed: 21281474]

62. Imachi H, Murao K, Hiramine C, Sayo Y, Sato M, Hosokawa H, Ishida T, Kodama T, Quehenberger O, Steinberg D, Takahara J. Human scavenger receptor B1 is involved in

recognition of apoptotic thymocytes by thymic nurse cells. Lab Invest. 2000; 80:263–270. [PubMed: 10701695]

63. Bannenberg GL, Chiang N, Ariel A, Arita M, Tjonahen E, Gotlinger KH, Hong S, Serhan CN. Molecular circuits of resolution: formation and actions of resolvins and protectins. J Immunol. 2005; 174:4345–4355. [PubMed: 15778399]
64. Gundra UM, Girgis NM, Ruckerl D, Jenkins S, Ward LN, Kurtz ZD, Wiens KE, Tang MS, Basu-Roy U, Mansukhani A, Allen JE, Loke P. Alternatively activated macrophages derived from monocytes and tissue macrophages are phenotypically and functionally distinct. Blood. 2014; 123:e110–122. [PubMed: 24695852]
65. Murray PJ, Allen JE, Biswas SK, Fisher EA, Gilroy DW, Goerdt S, Gordon S, Hamilton JA, Ivashkiv LB, Lawrence T, Locati M, Mantovani A, Martinez FO, Mege JL, Mosser DM, Natoli G, Saeij JP, Schultze JL, Shirey KA, Sica A, Suttles J, Udalova I, van Ginderachter JA, Vogel SN, Wynn TA. Macrophage activation and polarization: nomenclature and experimental guidelines. Immunity. 2014; 41:14–20. [PubMed: 25035950]
66. Adamson SE, Griffiths R, Moravec R, Senthivinayagam S, Montgomery G, Chen W, Han J, Sharma PR, Mullins GR, Gorski SA, Cooper JA, Kadl A, Enfield K, Braciale TJ, Harris TE, Leitinger N. Disabled homolog 2 controls macrophage phenotypic polarization and adipose tissue inflammation. J Clin Invest. 2016; 126:1311–1322. [PubMed: 26927671]
67. Ivashkiv LB. Epigenetic regulation of macrophage polarization and function. Trends Immunol. 2013; 34:216–223. [PubMed: 23218730]
68. Zizzo G, Hilliard BA, Monestier M, Cohen PL. Efficient clearance of early apoptotic cells by human macrophages requires M2c polarization and MerTK induction. J Immunol. 2012; 189:3508–3520. [PubMed: 22942426]
69. Venosa A, Malaviya R, Choi H, Gow AJ, Laskin JD, Laskin DL. Characterization of Distinct Macrophage Subpopulations during Nitrogen Mustard-Induced Lung Injury and Fibrosis. Am J Respir Cell Mol Biol. 2016; 54:436–446. [PubMed: 26273949]
70. Luan B, Yoon YS, Le Lay J, Kaestner KH, Hedrick S, Montminy M. CREB pathway links PGE2 signaling with macrophage polarization. Proc Natl Acad Sci USA. 2015; 112:15642–15647. [PubMed: 26644581]
71. Keravis T, Monneaux F, Yougbare I, Gazi L, Bourguignon JJ, Muller S, Lugnier C. Disease progression in MRL/lpr lupus-prone mice is reduced by NCS 613, a specific cyclic nucleotide phosphodiesterase type 4 (PDE4) inhibitor. PloS one. 2012; 7:e28899. [PubMed: 22247763]
72. De Souza A, Strober BE, Merola JF, Oliver S, Franks AG Jr. Apremilast for discoid lupus erythematosus: results of a phase 2, open-label, single-arm, pilot study. J Drugs Dermatol. 2012; 11:1224–1226. [PubMed: 23134988]

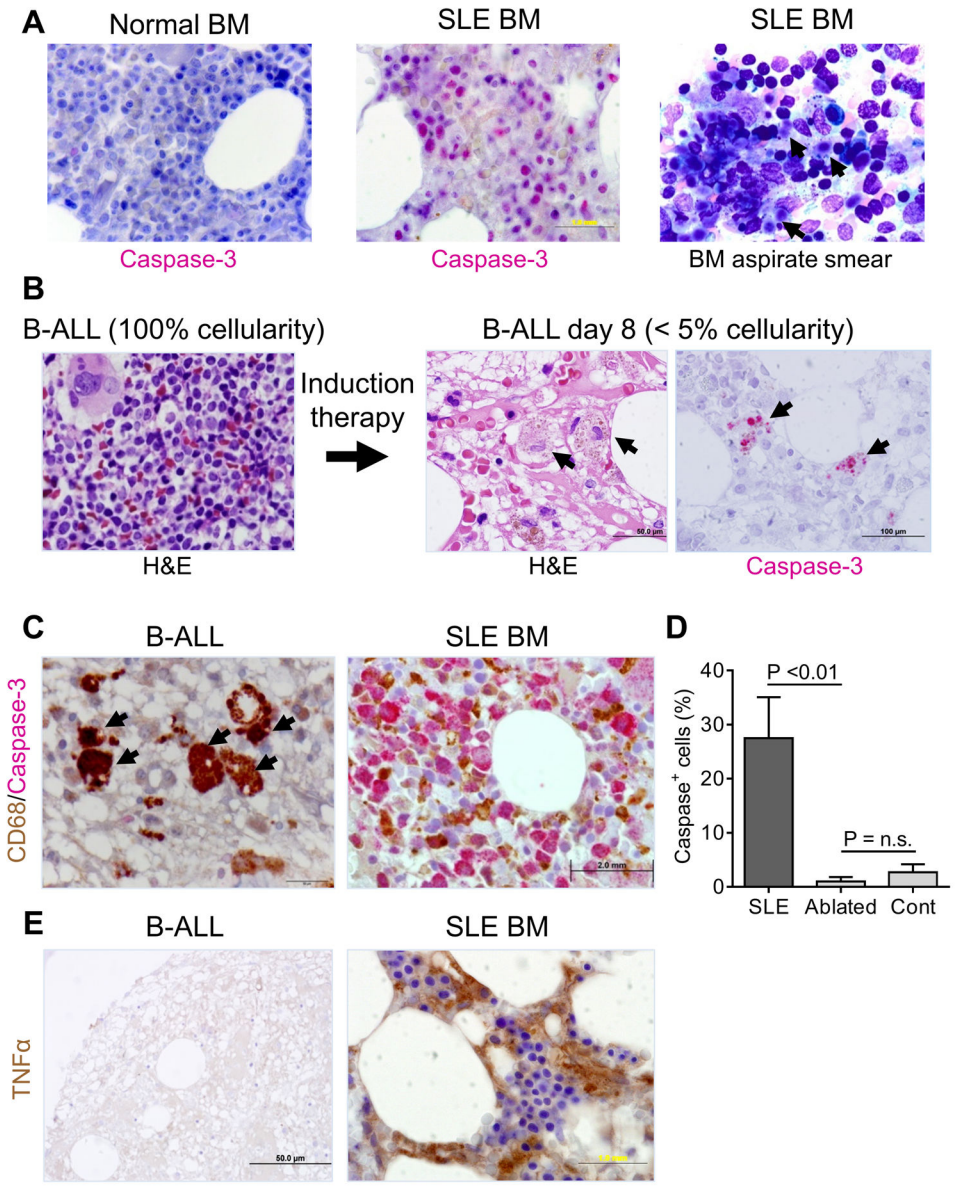

Figure 1. Immunohistochemistry (IHC) for dead cells human bone marrow (BM)

A, Double IHC staining (*left* and *middle*) of BM from a patient with SLE vs. a control with idiopathic thrombocytopenic purpura using anti-CD68 (brown) and anti-activated caspase-3 antibodies (red). *Right*, BM aspirate smear from an SLE patient showing the presence of uncleared dead cells (arrows, Wright-Giemsa stain). **B,** Hematoxylin and eosin (H&E) staining of BM core biopsies from a patient with B cell ALL (B-ALL) prior to myeloablation (100% cellularity, *left*) and 8-days after chemotherapy (<5% cellularity, *middle*). Arrows show macrophages that have taken up cellular debris. *Right*, IHC of day-8 BM using anti-activated caspase-3 antibodies (red). Arrows show activated caspase-3^{+} material inside macrophages. **C,** double IHC of BM core biopsies from the B-ALL patient (post-myeloablation, *left*) and from an SLE patient (*right*) for activated caspase-3 (red) and CD68 (brown). Arrows (left) show caspase-3/CD68 double positive cells. **D,** percentages of

activated intact caspase-3 positive cells (IHC) located outside of macrophages in BM from patients undergoing myeloablation (Ablated, n = 4) vs. SLE patients (n = 6) and controls (Cont, n = 6) ($P < 0.01$ ablated vs. SLE; P = not significant (n.s.) ablated vs. controls (Mann-Whitney). **E,** IHC of BM from the post-myeloablation B-ALL patient (*left*) and an SLE patient (*right*) for TNFα (brown). H&E and IHC staining patterns shown are representative of 4 patients undergoing myeloablation, 6 with SLE, and 6 healthy controls.

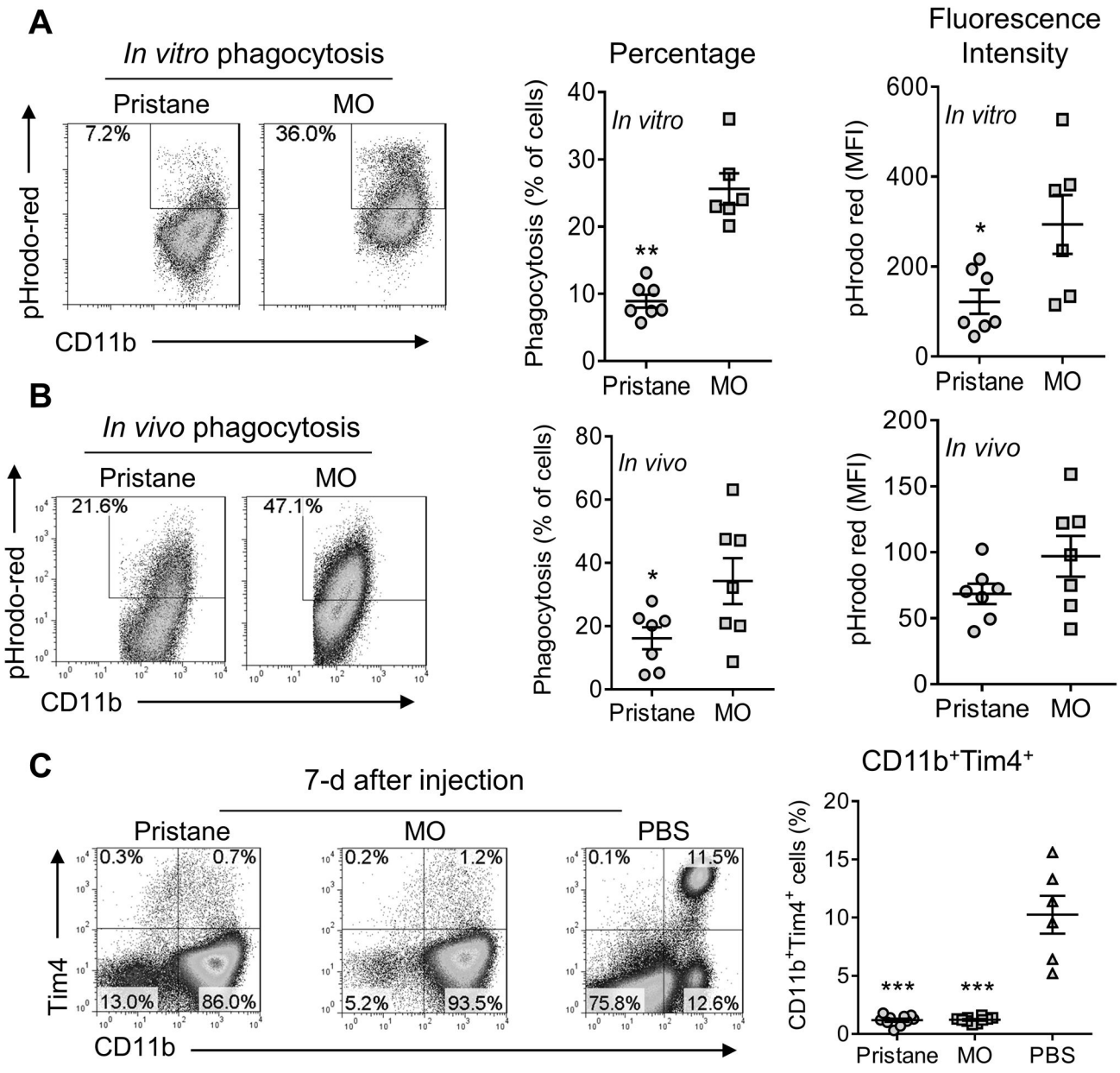

Figure 2. Phagocytosis of apoptotic cells in the peritoneum

A, *in vitro* phagocytosis of pHrodo-labeled apoptotic BW5147 cells by $CD11b^+$ cells from pristane-treated vs. mineral oil (MO)-treated B6 mice. **B,** *in vivo* phagocytosis of pHrodo-labeled apoptotic BW5147 cells by $CD11b^+$ cells from pristane-treated vs. MO-treated mice. **C,** peritoneal cells from mice treated 7-days earlier with pristane, MO, or PBS, were stained with anti-CD11b and anti-Tim4, and analyzed by flow cytometry. Percentages of peritoneal $CD11b^+Tim4^+$ cells in pristane, MO, and PBS treated mice are shown on the right. *, $P < 0.05$; ** $P < 0.01$; *** $P < 0.001$ (2-tailed t-test).

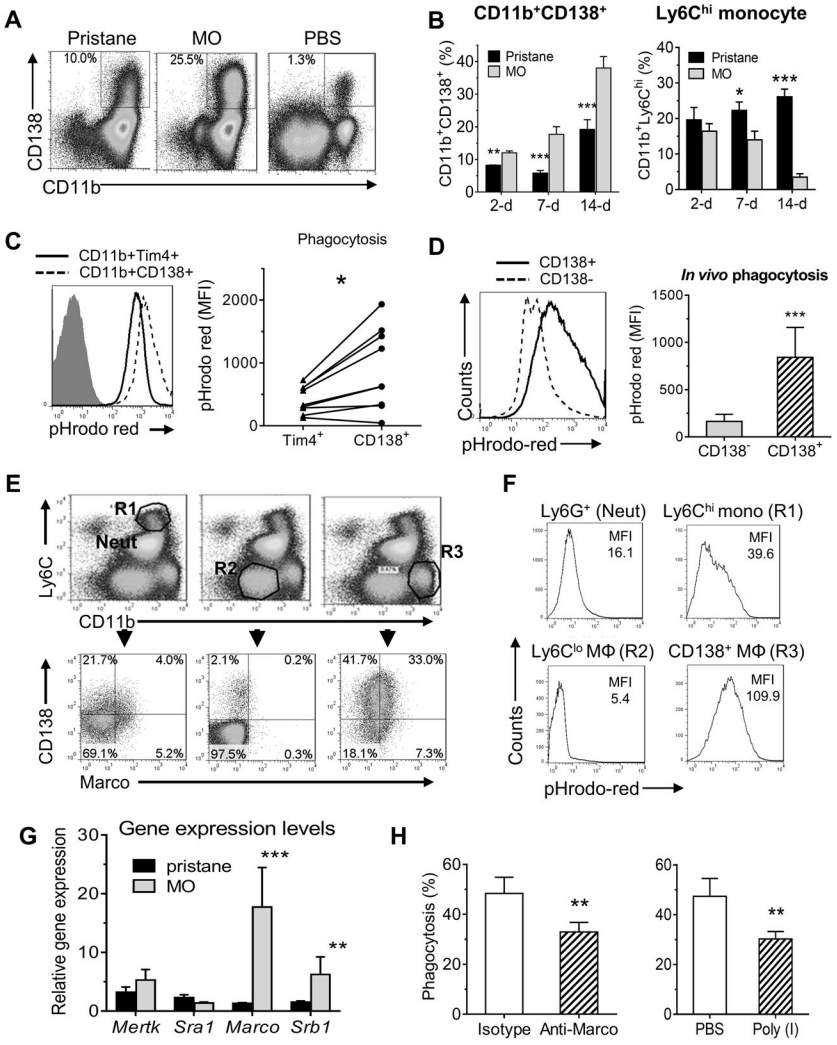

Figure 3. Depletion of CD11b$^+$Tim-4$^+$ resident Mϕ and expansion of CD11b$^+$CD138$^+$ cells due to peritoneal inflammation

B6 mice were injected i.p. with pristane, mineral oil (MO), or saline (PBS) and peritoneal cells were collected at 7-days and stained with anti- CD11b, Tim-4, and CD138 monoclonal antibodies followed by flow cytometry. **A,** flow cytometry of peritoneal cells 1-week after pristane, MO, or PBS treatment stained with anti-CD11b and CD138 monoclonal antibodies. **B,** percentages of CD11b$^+$CD138$^+$ cells and CD11b$^+$Ly6C^{hi} monocytes in the peritoneum 2, 7, and 14 days after i.p. injection with pristane or MO. **C**, *in vivo* phagocytosis of pHrodo red-labeled apoptotic cells by peritoneal cells from untreated mice. Cell subsets were defined by staining with anti-CD11b, Tim4 and CD138 antibodies. Phagocytosis by the CD11b$^+$CD138$^+$ and CD11b$^+$Tim4$^+$subsets were compared. Graph at the right shows phagocytosis by the CD11b$^+$CD138$^+$ and CD11b$^+$Tim4$^+$ subsets from individual mice. **D,** *in vivo* phagocytosis of pHrodo red-labeled apoptotic cells by peritoneal cells from MO-treated mice. Cells were stained with anti-CD11b, Ly6G and CD138 antibodies. Gating on the CD11b$^+$ Ly6G$^-$ subset, phagocytosis of pHrodo-red-labeled apoptotic cells by CD138$^+$ vs. CD138$^-$ cells was compared. **E,** flow cytometry of peritoneal cells 1-week after MO

treatment of BALB/c mice using anti-CD11b, Ly6C, CD138, Ly6G and Marco antibodies. Cell subsets were defined by surface markers: neutrophils (Neut): $CD11b^{+}Ly6C^{int}$; $Ly6C^{hi}$ monocytes (R1): $CD11b^{+}Ly6C^{hi}$; $Ly6C^{lo}$ Mϕ, (R2): $CD11b^{+}Ly6C^{+/-;}$ $CD11b^{+}CD138^{+}$ cells (R3), $CD11b^{+}Ly6C^{+/-}$ $CD138^{+}$. Representative of five BALB/c mice (similar results were obtained in five B6 mice, not shown). **F**, *in vivo* phagocytosis of pHrodo red-labeled apoptotic cells by peritoneal cells from MO-treated BALB/c mice. After co-culture for 1.5-h with labeled-apoptotic targets, the cells were stained and gated as in **E**. Uptake of pHrodo-red-labeled apoptotic cells by neutrophils (neut), and the R1, R2, and R3 populations was compared. **G,** Levels of mRNA encoding phagocytosis-related genes in peritoneal cells from pristane-treated vs. MO-treated mice. **H,** *in vivo* phagocytosis of pHrodo red-labeled apoptotic BW5147 cells by peritoneal $CD11b^{+}$ cells from MO-treated mice injected i.p. 1-week later with rat anti-mouse Marco neutralizing antibodies or isotype control (100 μg/mouse, left) or treated i.p. with poly-inosinic acid (PolyI, 200 μg/mouse) or saline (PBS, right). *, $P < 0.05$; ** $P < 0.01$; *** $P < 0.001$ (2-tailed t-test).

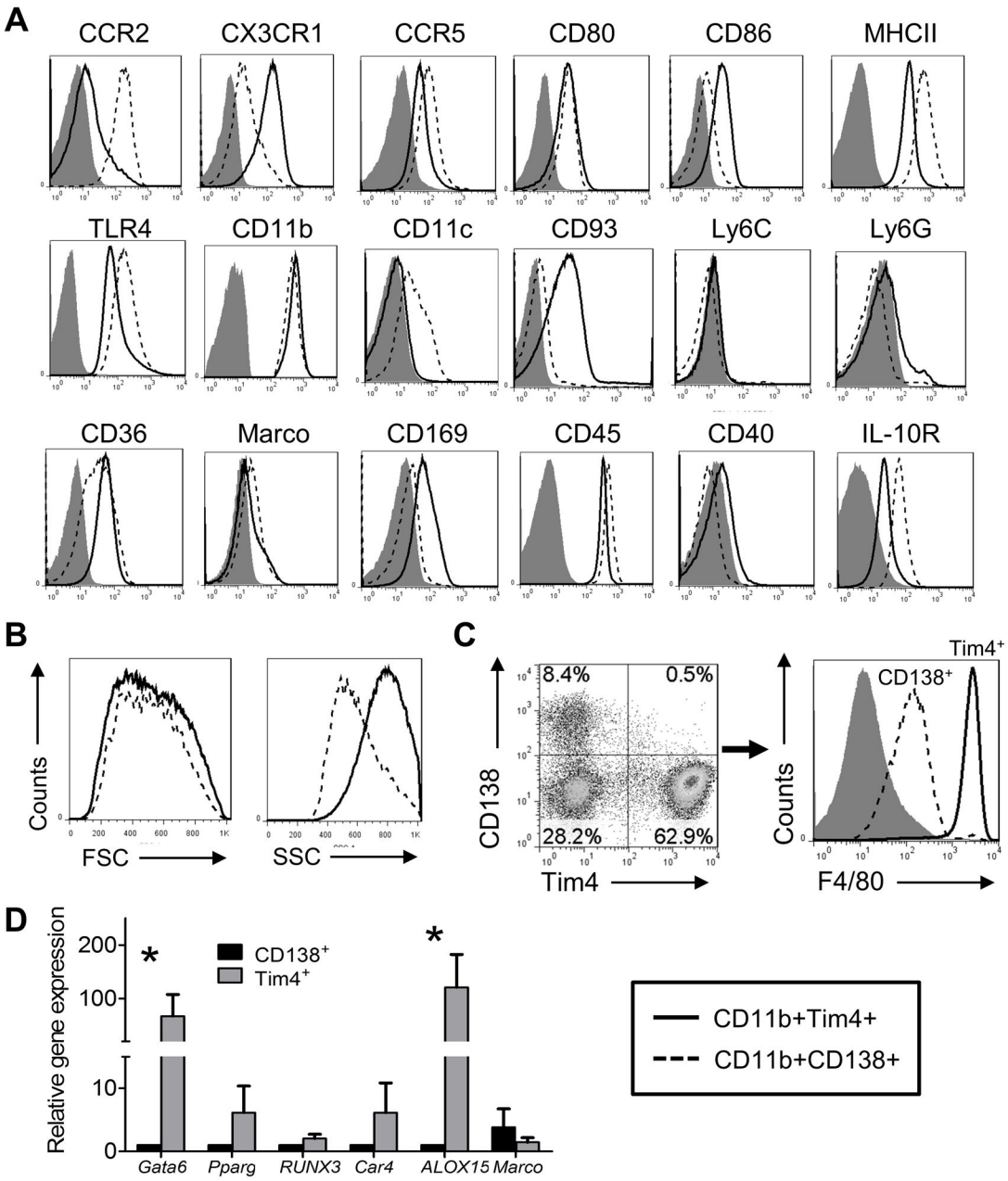

Figure 4. Comparison of the CD11b$^+$CD138$^+$ and CD11b$^+$Tim4$^+$subsets

A, peritoneal cells from untreated B6 mice were stained with F4/80 plus anti- CD11b, CD138 and Tim4 monoclonal antibodies and gated on CD11b$^+$ cells. CD11b$^+$CD138$^+$ and CD11b$^+$Tim4$^+$subsets were analyzed for surface marker expression (flow cytometry). Isotype control: filled curve; CD11b$^+$CD138$^+$ subset: dashed line; CD11b$^+$Tim4$^+$subset: solid line. **B,** forward (FSC, size) and side (SSC, complexity) scatter characteristics of the CD11b$^+$CD138$^+$ and CD11b$^+$Tim4$^+$subsets. **C,** peritoneal cells from untreated mice were stained with anti- CD11b, Tim-4, CD138, and F4/80 monoclonal antibodies followed by flow cytometry, gating on CD11b$^+$ cells. Percentages of CD11b$^+$Tim4$^+$CD138$^-$ and CD11b$^+$Tim4$^-$ CD138$^+$ cells (*left*), and fluorescence intensity of F4/80 staining (*right*) are

shown (representative of 10 mice). **D,** peritoneal $CD11b^{+}Tim4^{+}$ and $CD11b^{+}CD138^{+}$ cells from untreated mice were flow-sorted and gene expression was compared by real-time PCR using mRNA isolated from each subset. *, $P < 0.05$ (2-tailed t-test).

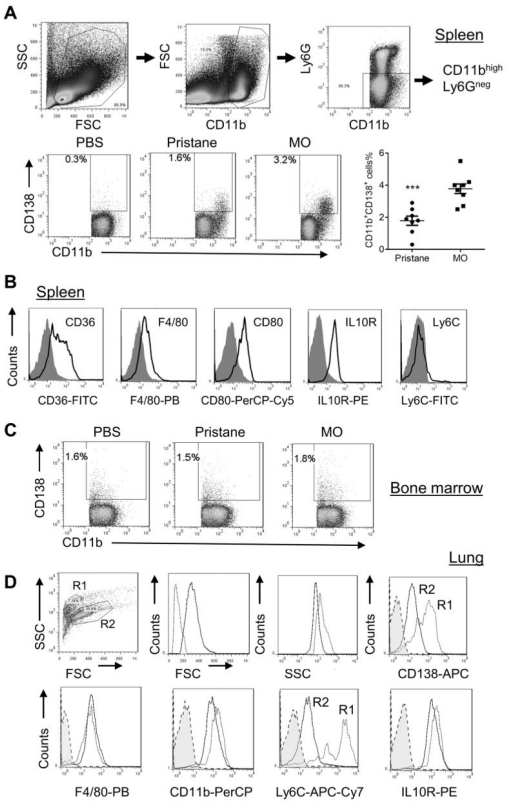

Figure 5. CD11b^{+}CD138^{+} Mϕ subset is present in spleen, lung and bone marrow

A, spleen cells from PBS, pristane and MO treated B6 mice were stained with anti- CD11b, CD138, and Ly6G. Cell subsets were defined by surface markers. Percentages of CD11b^{+}CD138^{+} cells were compared in different treatment groups. **B,** spleen CD11b^{+}CD138^{+} cells from MO treated mice were analyzed for CD36, F4/80, CD80, IL-10R, and Ly6C expression. **C,** bone marrow CD11b^{+}CD138^{+} cells were compared in different treatment groups. **D,** lung CD11b^{+}CD138^{+} cells from MO treated mice were analyzed for CD138, F4/80, CD11b, Ly6C, and IL-10 receptor (IL10R) surface staining (flow cytometry). R1, small CD138^{hi}Ly6C^{hi}F4/80^{+} Mϕ; R2, large CD138^{lo}Ly6C^{lo}F4/80^{+} alveolar Mϕ. *** $P < 0.001$ (2-tailed t-test).

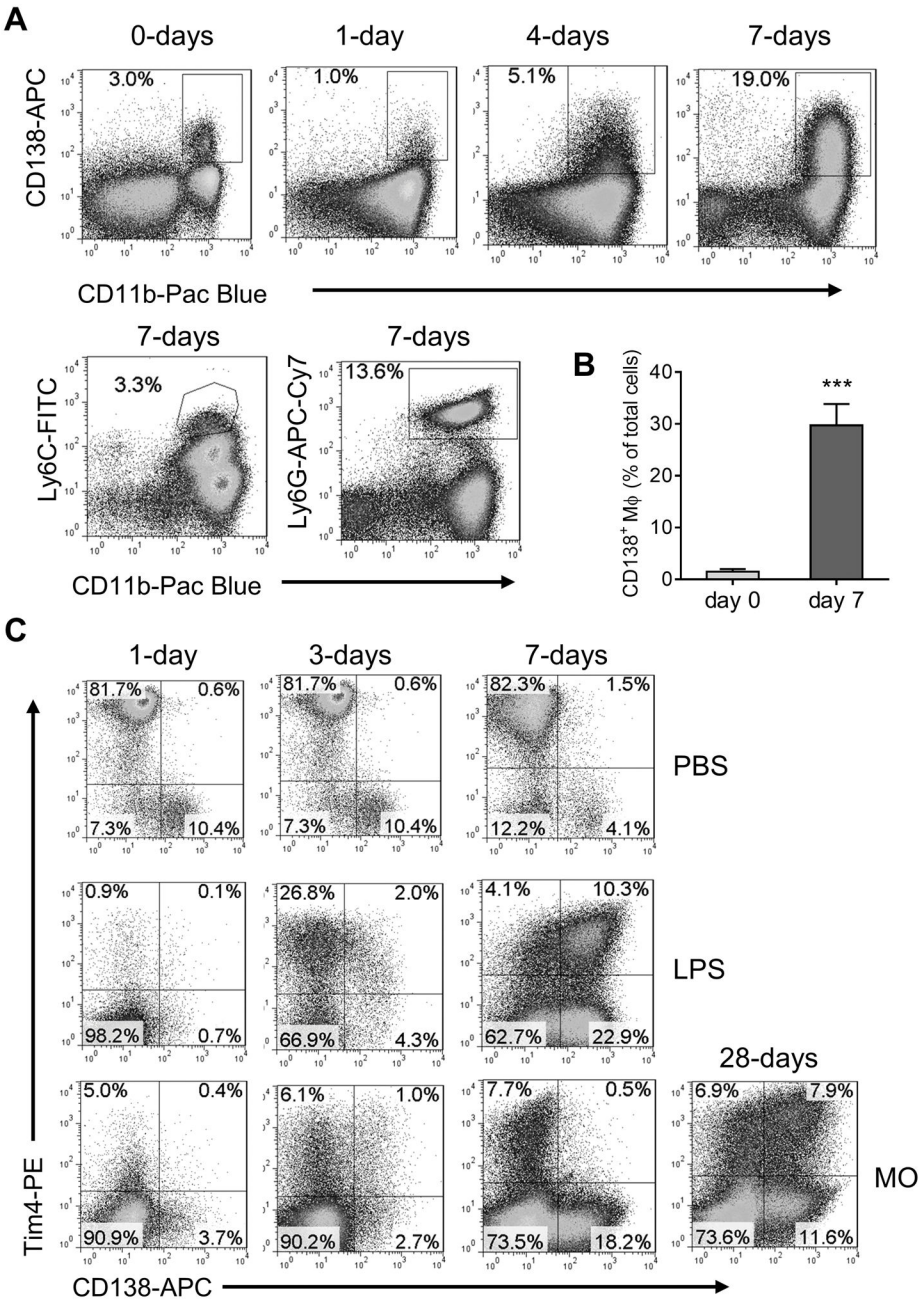

Figure 6. CD11b^{+}CD138^{+} Mϕ subset is induced by lipopolysaccharide (LPS)

B6 mice were injected with LPS (100 ng i.p.) and peritoneal cells were analyzed by flow cytometry 0–7 days later for CD138 and CD11b (top four panels) or Ly6C and CD11b (bottom two panels). **A,** Staining of peritoneal cells from LPS treated mice with anti-CD11b, anti-CD138, anti-Ly6C, and Ly6G antibodies. **B,** CD138^{+} Mϕ in B6 mice before (day 0) and 7-days after LPS treatment. **C,** flow cytometry of peritoneal cells from PBS (0.5 ml i.p., top row), LPS (100 ng i.p. in PBS, middle row), and MO (0.5 ml i.p., bottom row) treated BALB/c mice with anti-CD138 and -Tim4 antibodies (days 1–28). *** $P < 0.001$ (2-tailed t-test).

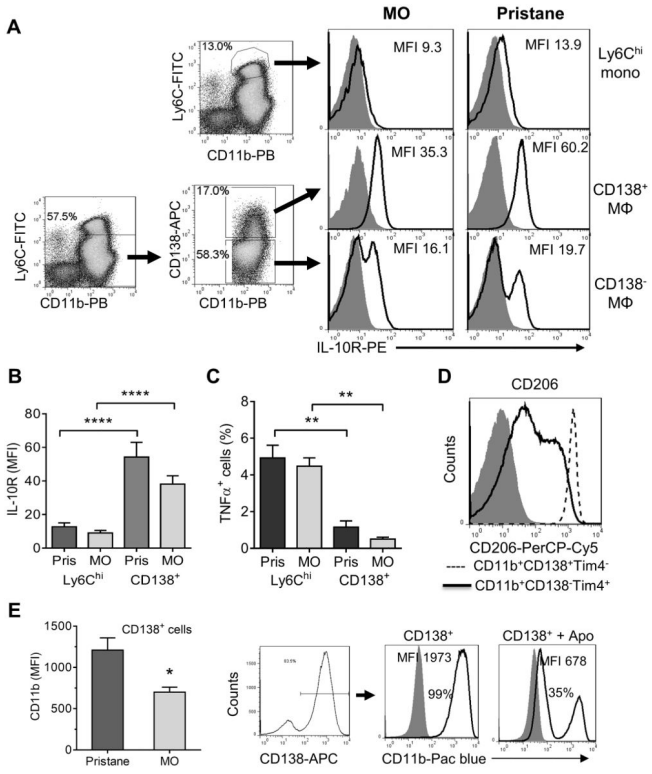

Figure 7. CD11b$^+$CD138$^+$ Mϕ subset has an anti-inflammatory phenotype

A, IL-10R expression (mean fluorescence intensity, MFI) in different cell subsets of peritoneal cells from pristane and MO treated B6 mice (1-week after IP injection). Ly6C^{hi} monocytes (Ly6C^{hi}CD11b$^+$); CD138$^+$ Mϕ (Ly6C$^{lo/-}$ Ly6G$^-$ CD11b$^+$CD138$^+$); CD138$^-$ Mϕ (Ly6C$^{lo/-}$ Ly6G$^-$ CD11b$^+$CD138$^-$). **B,** quantification of IL-10 receptor (IL-10R) expression in Ly6C^{hi} monocytes vs. CD138$^+$ Mϕ from pristane and MO treated mice. Gating for Mϕ subsets was done as in **A. C,** comparison of intracellular TNFα staining in CD11b$^+$Ly6C^{hi} monocytes (Ly6C^{hi}) and the CD11b$^+$CD138$^+$ Mϕ subset (CD138$^+$) from pristane and MO treated mice. **D**, CD206 staining. Peritoneal cells from untreated B6 mice were stained with antibodies against CD11b, Tim4, CD138 and CD206. CD206 staining was compared between the CD11b$^+$CD138$^+$ (dashed line) and CD11b$^+$Tim4$^+$subsets (solid line). Isotype control: filled curve. **E,** CD11b expression is down-regulated by uptake of apoptotic cells. *Left,* CD11b staining of CD138$^+$ cells from pristane vs. MO-treated mice. *Right,* effect of apoptotic cells on CD11b expression on CD138$^+$ Mϕ from MO-treated mice. Flow-sorted CD138$^+$ Mϕ were co-cultured for 20-h with apoptotic BW5147 cells (5:1 ratio apoptotic cells to Mϕ) and fluorescence intensity of CD138 was determined on the CD138$^+$ Mϕ by flow cytometry. Shaded curve, isotype control. *, P < 0.05; ** P < 0.01; **** P < 0.0001 (2-tailed t-test).

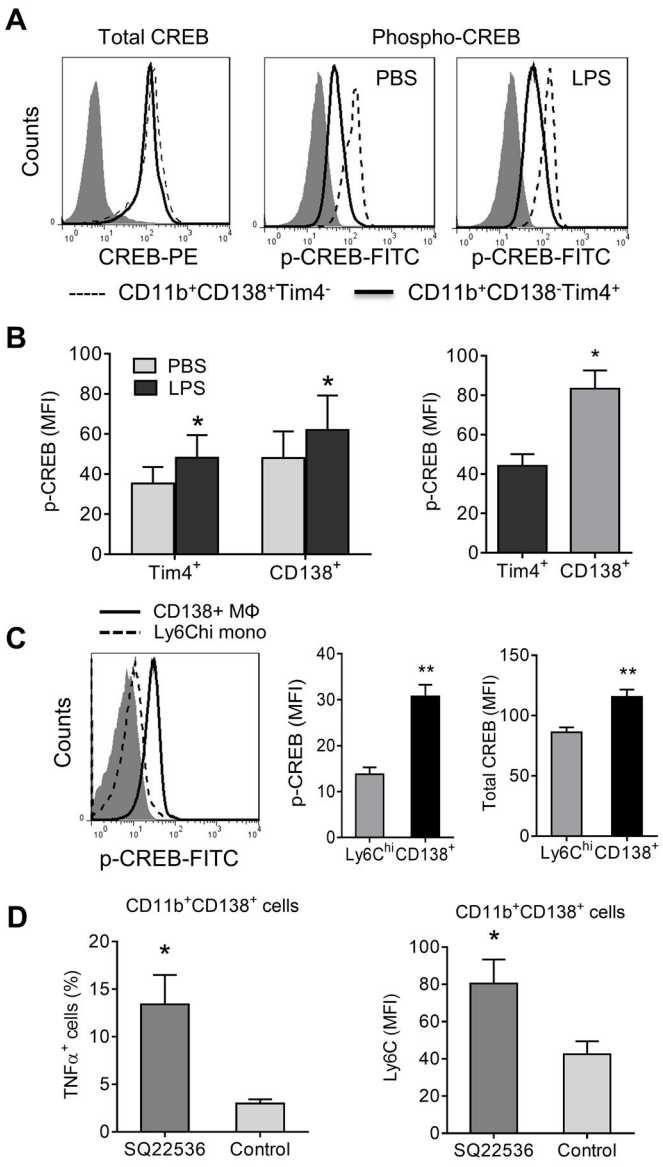

Figure 8. CREB activation

A, Flow cytometry of total CREB and activated (p-CREB) staining. Peritoneal cells from untreated B6 mice were incubated with PBS or LPS (100 ng/ml) for 30 min. Total CREB and phosphorylated CREB (p-CREB) staining was compared between the $CD11b^{+}CD138^{+}Tim4^{-}$ (dashed line) and $CD11b^{+}CD138^{-}$ $Tim4^{+}$subsets (solid line). Isotype control: filled curve. **B,** p-CREB levels in $CD11b^{+}CD138^{+}Tim4^{-}$ and $CD11b^{+}CD138^{-}$ $Tim4^{+}$ cells from untreated mice. Data are representative of five separate experiments, total 20 mice. **C,** Activated CREB in $Ly6C^{hi}$ monocytes vs. $CD138^{+}$ Mϕ. *Left,* comparison of p-CREB staining by flow cytometry in $Ly6C^{hi}$ monocytes (dashed line) and $CD138^{+}$ Mϕ (solid line) from MO treated mice. *Middle*, p-CREB staining (mean fluorescence intensity, MFI) of $Ly6C^{hi}$ monocytes vs. $CD138^{+}$ Mϕ. *Right*, total CREB staining (MFI) of $Ly6C^{hi}$ monocytes vs. $CD138^{+}$ Mϕ. **D,** Effect of adenylate cyclase inhibition. Mice were treated with MO (0.5 ml i.p.) plus either SQ22536 (250 μg i.p. daily) or vehicle. At day 9,

peritoneal exudate cells were surface stained for CD11b, CD138, Ly6C, and intracellularly stained for TNFα. The percentage of $CD11b^{+}CD138^{+}$ cells positive for TNFα (left) and the MFI of Ly6C staining (right) was determined by flow cytometry. *, $P < 0.05$; ** $P < 0.01$ (2-tailed t-test).